# Time-Elapse Communication: Bacterial communication on a microfluidic chip

Bhuvana Krishnaswamy [a], Caitlin M. Austin [b], J. Patrick Bardill [c], Daniel Russakow [b], Gregory L. Holst [b], Brian K. Hammer [c], Craig R. Forest [b], Raghupathy Sivakumar [a]

[a] School of Electrical and Computer Engineering, [b] George W. Woodruff School of Mechanical Engineering
[c] School of Biology,
Georgia Institute of Technology, Atlanta, GA, USA

***Abstract*—**

**Bacterial populations housed in microfluidic environments can serve as transceivers for molecular communication, but the data-rates are extremely low (e.g., $10^{-5}$ bits per second.). In this work, genetically engineered *Escherichia coli* bacteria were maintained in a microfluidic device where their response to a chemical stimulus was examined over time. The bacteria serve as a communication receiver where a simple modulation such as on-off keying (OOK) is achievable, although it suffers from very poor data-rates. We explore an alternative communication strategy called time-elapse communication (TEC) that uses the time period between signals to encode information. We identify the limitations of TEC under practical non-zero error conditions and propose an advanced communication strategy called smart time-elapse communication (TEC-SMART) that achieves over a 10x improvement in data-rate over OOK. We derive the capacity of TEC and provide a theoretical maximum data-rate that can be achieved.**

***Index Terms*—Molecular communication, On-Off Keying, Time Elapse Communication**

## I. Introduction

Nano-scale communication strategies can be categorized into two broad domains depending upon their target environment: *electromagnetic communication (EM)* at the nano-scale involves the extension of traditional EM based communication techniques for use in inorganic or non-biological applications [1], [2]; and *molecular communication* involves strategies (typically bio-inspired) for use in biological applications [3]–[6]. In recent years, bacteria have emerged as promising candidates for nano-machines in biological applications [7]. Bacteria are prokaryotic microorganisms, typically about 1 $\mu$m in size, that are well-studied and understood in terms of morphology, structure, behavior, and genetics. Genetic engineering of bacteria to introduce or delete DNA for specific traits (e.g., bioluminescence, motility, adhesion, etc.) has enabled recent advancements in synthetic biology [8]. Many bacteria utilize a process called quorum sensing, whereby bacterial cells naturally behave as transceivers that interact with one another, relaying signals by transmitting and receiving chemical signal molecules [9], [10]. Using the power of synthetic biology and the inherent transceiver properties, bacterial nano-machines hold much promise to be used in biological applications such as toxicology, biofouling, and biosensing. For example, receiver bacteria have been used as biosensors to detect the presence of metals [11], and to detect arsenic pollution [12].

*The context for this work is thus molecular communication between bacterial populations.* Specifically, we consider a system in which bacterial populations are used as transceivers connected through microfluidic pathways for molecular signals. The focus of this work is to study the communication performance between the transceivers and develop strategies to improve the same. To this end, we make three major contributions:

First, we use *Escherichia coli (E. coli)* bacteria genetically engineered to exhibit fluorescence upon the receipt of a specific signal molecule (N-(3-Oxyhexanoyl)-L-homoserine lactone, or C6-HSL). A microfluidic experimental system houses bacterial populations within micrometer sized chambers fed

This work was supported in part by the National Science Foundation under grant CNS-1110947. A shorter version of this paper appeared in the Proceedings of the 2013 IEEE International Conference on Communications.

by channels that provide both nutrients and controllable levels of C6-HSL, to demonstrate that a chemical signal at the sender can be reproduced as a fluorescence signal at the receiver reliably. Specifically, we demonstrate that it is indeed feasible to realize a simple modulation technique such as *On-Off Keying* ($OOK$) for communication between the bacterial populations, but the consequent data rates achievable is as low as $10^{-5}$ bps. We term such environments where the transmission rates are very low as *super-slow networks*.

Second, we introduce a new communication strategy called *time-elapse communication* ($TEC$) for *super-slow networks* that relies on the time interval between two signals to encode information. Thus offloading some of the communication burden to the sender and receiver (in the form of measuring time periods), we show that *TEC* under idealized conditions can deliver data-rate improvements of an order of magnitude in the target environment. We also evaluate $TEC$ under realistic conditions that involve non-zero error and show that the performance of $TEC$ reduces to being marginally better than $OOK$. We propose an improved communication strategy called *smart time-elapse communication* ($TEC$-$SMART$) that improves data-rate performance in realistic non-zero timing error conditions. $TEC$-$SMART$ is a combination of two mechanisms viz., **Error Differentiation** and **Differential Coding** where the former decouples different components of timing error, and corrects each component differently and the second component reduces total delay by transmitting difference of adjacent messages.

Third, we derive the maximum achievable capacity using time based communication like $TEC$. We present an analysis of capacity for different distribution of noise viz., a uniformly distributed noise and an exponentially distributed noise in the microfluidic channel. Using simulations driven by experimental data, we also show that $TEC$-$SMART$ approaches the original promise of $TEC$ even under realistic conditions involving non-zero error. We identify data-rate as a function of different parameters and perform a sensitivity analysis to analyze the impact of each parameter.

The rest of the paper is organized as follows: Section II presents a detailed description of the bacterial strain used and the microfluidic system that houses the bacteria. Section III presents the results from microfluidic experiments with *E. coli* bacteria and establishes the motivation for $TEC$ in *super-slow networks*. Section IV presents the key design principles of $TEC$. Section V presents the theoretical maximum achievable data-rate using $TEC$ and Section VI presents the simulation results of $TEC$ along with the optimization proposed. Section VII presents related work and Section VIII concludes the paper.

## II. Experimental System Design

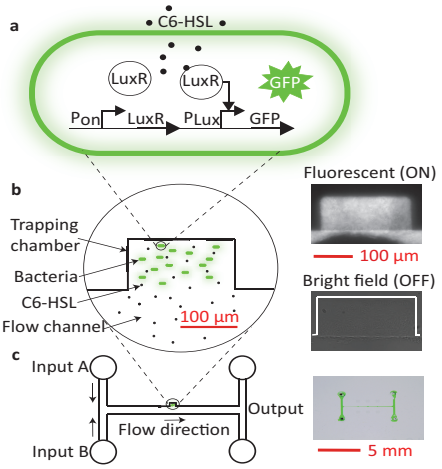


Fig. 1: (a) Genetically Engineered *E. coli* Bacteria (b) Bacteria are housed in rectangular trapping chambers that are in fluidic contact to the main flow channel. As C6-HSL flows through the main channel, the C6-HSL diffuses across the trapping chamber, which leads to the fluorescent response in the bacteria (fluorescent image inset). In the absence of C6-HSL, there is no fluorescence (bright field image).(c) Two inputs and two outputs are used in the microfluidic device adapted from Danino et al. [7]. (Photo of microfluidic device inset.)

In this work, we consider a system in which genetically engineered bacterial populations are used as transceivers connected through microfluidic pathways. Microfluidic pathways allow for dynamic changes in media composition. Further, the constant stream of media keeps the bacteria in ideal growth conditions, eliminating growth phase dependent variables from the experiments.

### A. Genetically Engineered E. coli Bacteria

We set out to establish an experimental system for testing the foundations of molecular based communication in bacteria. To do this we utilized a marine symbiotic bacterium *Vibrio fischeri (V. fischeri)* which possesses a quorum sensing system

called the LuxIR circuit. In standard laboratory conditions, the LuxIR circuit causes *V. fischeri* to generate light when a culture reaches an optical density $0.4$ at $600$ nM [13]. In the native system, the LuxI enzyme catalyzes the generation of a signaling molecule, C6-HSL. C6-HSL diffuses freely into and out of the bacterial cell. In the bacterial cell, C6-HSL binds with a second component, the LuxR receptor. LuxR, in complex with C6-HSL, binds specific DNA sequences and activates transcription of genes that are responsible for light production. In the native organism each individual cell serves as both a transmitter and receiver of signal. However, we ectopically expressed part of the LuxIR circuit in the model bacterial organism *E. coli* to engineer cells that only behave as receivers of signals. Specifically, we introduced into *E. coli* a plasmid that constitutively produced the LuxR receptor protein.

Standard microbiological techniques were used in the culturing of *E. coli*. All experiments were performed in 2xYT broth [14]. *E. coli* strain DH5$\alpha$ was used for all cloning. Receiver bacteria were derived from the fully sequenced K-12 strain MG1655 [15]. To generate the receiver plasmid, Biobrick BBa_T9002 (partsregistry.org) was modified using PCR based methods to append a $ssrA$-degradation tag (ANDENYALAA) to the C-terminus of green fluorescent protein (GFP) [16]. The resulting plasmid was transformed into MG1655 to create the receiver bacteria. The resulting strain exhibits fluorescence upon the receipt of a specic signal molecule C6-HSL, and is depicted schematically in Figure 1(a). When C6-HSL is added to the fluidic platform, it enters the receiver *E. coli* cells, LuxR complexes with C6-HSL and then binds to DNA sequences that induce transcription of an unstable variant of Green Fluorescent Protein (GFP) (Figure 1(a)). A constitutive promoter ($P_{on}$) that is always on drives expression of the *luxR* gene that codes for the C6-HSL receptor, LuxR. When the C6-HSL signal reaches the receiver cells, it diffuses into the cell, and binds to LuxR. The LuxR/C6-HSL complex activates the *lux* promoter (PLux), resulting in expression of the GFP gene carrying a degradation tag, and production of green fluorescent protein (GFP). Engineered in this manner, receiver cells will become fluorescent in response to C6-HSL, and will stop being fluorescent when C6-HSL is no longer present.

### *B. Microfluidic System*

Several other groups have examined responses of a bacteria to stimuli either in bulk culture or in a microfluidic environment [17]. In [18], the effect of population density on the ability of bacteria to respond was examined in microtiter plate wells. The effects of flow on receiver bacteria was examined in a microfluidic device in [19]. However, since poly-L-lysine was the method used to contain bacteria populations, experiments were limited to only to a few hours. Communication between two bacterial populations over time has been examined in [20] through means of a micro-ratchet structure and self-regulating populations that act as oscillators [7], [21]. Delivering a chemical stimulus in a time varying manner to a microfluidic bacteria while monitoring the fluorescent response was done previously by Groisman et al. [22]. In the current work, we advance this method by exploring the fundamental limits of pulse width. We modulate input signal using chemical cues to measure fundamental performance limits and ultimately to develop a new method of encoding molecular information surpassing these limits such that the data-rate is dramatically improved over $OOK$, the simplest form of amplitude shift keying wherein the presence of a signal (ON) represents a 1, and the absence (OFF) represents a 0.

Figure 1(c) shows an illustration of the microfluidic device. To fabricate it, we utilized standard soft lithography [23] with polydimethyl siloxane (PDMS) bonded to a glass coverslip. Briefly, PDMS (1:10) was cast on an $SU$-$8$ mold, plasma treaded with the grade $1.1$ coverslip for $1.5$ min, and bonded immediately following.

During experiments, bacteria were maintained in chambers on the device (see Figure 1(b)) while bacterial growth medium (2xYT media containing ampicillin at 10 $\mu$g/ml) was delivered to flow channels alternatively with medium containing C6-HSL signal (note inlet A and B in Figure 1c). The central flow channel (250 $\mu$m wide x 10 $\mu$m high) is in direct fluidic contact with the chamber (150 $\mu$m x 100 $\mu$m x 5 $\mu$m high) as shown in Figure 1(b),(c). In response to C6-HSL, the bacteria fluoresce (see Figure 1(b)), as imaged on a fluorescence microscope (Nikon TE 2000), with stage heated to (30°C). The microfluidic system included the microfluidic device on the microscope stage, pumps

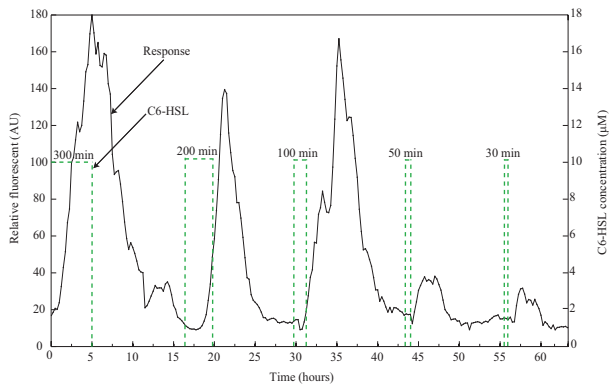


(a) Bacteria relative fluorescence was measured in response to varying pulse inputs (300, 200, 100, 50 and 30 min) of C6-HSL. A typical response is shown.

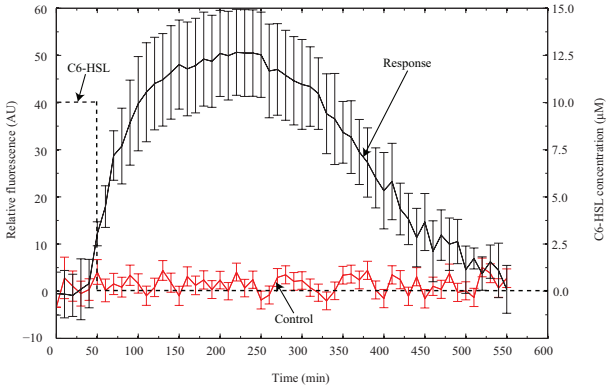


(b) Bacteria relative fluorescence was measured in response to pulse input of duration 50 min of C6-HSL (Number of experiments=10), as compared to a reference (Number of experiments=4). Error bars represent one standard deviation.

Fig. 2: Response of Bacteria to Input signal

and tubing. To initially load bacteria on the chip, cells were injected in media through one of the inlet ports using a syringe to fill the chip entirely. Excess bacteria were flushed away, Tygon tubing was attached between the chip and pumps using short metal tubes, and the chip was placed on the microscope stage. The bacteria were then allowed to populate the chamber for 24 hrs until it reached capacity, $\backsim 10^5$ bacteria per chamber, during which time both inlets were used to flow 2xYT media at 100 $\mu$l/hr using syringe pumps (Harvard Apparatus). This flow rate was empirically determined to allow the bacteria to successfully colonize the chambers without being washed away.

Once the bacteria had filled the trapping chamber, combined flow rate was increased to 360 $\mu$l/hr. Inlet B was used for 2xYT medium alone (at 350 $\mu$l/hr), while inlet A (10 $\mu$l/hr) was used to varying concentrations and durations of C6-HSL as noted. Fluorescence images during the course of the experiment (1/10 min) were processed using MATLAB. For three consecutive images, a region of interest was selected that encompassed the chamber, the intensity of the pixels was averaged, and the background fluorescence subtracted out, yielding the signal strength. The obtained signal strength is defined as the relative fluorescence(y-axis) in Figure 2(a) and 2(b). The signal-to-noise (SNR) was then computed as the signal strength divided by the standard deviation of the background noise (non fluorescent bacteria-filled chamber).

## III. Microfluidic Experimental Results using OOK

Using the genetically engineered bacteria in the microfluidic system in Figure 1(c), we were able to elicit a fluorescent response to C6-HSL and image it with the fluorescence microscope (Figure 1(b)). At steady state (e.g., 1 hr) we were able to image fluorescent bacteria (number of experiments=10, SNR=20), and return them to non-fluorescing state by removing C6-HSL from the flow channel (number of experiments=10, SNR$<$1). We experimented with modulating the C6-HSL input as a pulse with 10 $\mu$M concentration for a variety of durations. As shown in Figure 2(a), the bacteria responds differently to the varying input pulse with varying widths.

In order to select an appropriate input pulse width, an experiment was run with varying pulses of 10 $\mu$M C6-HSL to determine the minimum pulse width that fit our requirements for a distinguishable signal. To be considered as a signal, we define a threshold signal-to-noise ratio (SNR) as $\geq$ 5, and a plateau region of sustained fluorescence above this SNR threshold of duration greater than 10% of the total signal time. Shown in Figure 2(a), the bacteria were exposed for 300, 200, 100, 50 and 30 mins with periods of pure media in between. The 50 min pulse was the shortest pulse that met these requirements, and was therefore used in the following experiments. The bacteria were exposed to C6-HSL for a 50 min pulse for all results

shown in Figure 2(b). For ten samples, the average response time, defined as the time from when the bacteria begin to fluoresce until the time they stop, was found to be 435 min. with a standard deviation of 47. The average delay time, characterized as the time between when the bacteria start to receive the C6-HSL until they begin to fluoresce, was 31 min. with a standard deviation of 11. The average SNR was 7.9. We used the microfluidic system to demonstrate that $OOK$ is (a) achievable in the target environment; and (b) has a data-rate performance that is quite low.

*It can be seen that the receive signals clearly follow the ON-OFF patterns at the sending side, albeit offset by the propagation delay in the environment*. While the above results demonstrate that $OOK$ can indeed be relied upon for conveying information from the sender to the receiver, we now proceed to derive the achievable data-rates using $OOK$ based on parameters extracted from the experiments. The key parameter of interest in determining the achievable data-rate is the *bit period*. The bit period at the receiver is greater than that at the sending side due to the biological processing at the receiver bacteria. We define the maximum of the two bit periods as the effective bit period $t_b$. Acceptable SNR threshold used is an empirical value based on visual observation. The condition on SNR threshold determines the effective bit period ($t_b$) of the system. Therefore, we analyze different values of $t_b$ in our numerical analysis in Section VI. The data-rate of $OOK$ is thus $\frac{1}{t_b}$, which for a $t_b$ of 435 min is $3.8 * 10^{-5}$ bps. In the rest of the paper, we introduce and describe strategies that are aimed toward improving the achievable data-rates in *super-slow networks*.

## IV. Time-Elapse Communication

The data-rate performance of $OOK$ in bacterial communication is low due to the inordinately large bit period involved. Hence, in this paper we explore a communication strategy called *time- elapse communication* ($TEC$), wherein information is encoded in the time period between two consecutive signals. A pictorial representation of $TEC$ and $OOK$ is presented in Figures 3(a) and 3(b). The number of molecular signals generated always remains at two (the start and the stop) irrespective of the number of bits required to represent the information. $TEC$ requires the clock rates at the sender and receiver to be the same, although no clock synchronization is required. Intuitively, $TEC$ improves the data-rate over $OOK$ by reducing the number of communication signals that needs to be conveyed per unit of information.

More precisely, if the clock rate at the sender and receiver is $f_c$, information $v$ is represented by the sender as $v/f_c$ time units separating a *start* signal and a *stop* signal, where $v \in \mathbb{N}$. If the communication involves conveying a series of such values, the *stop* signal of a particular value is used as the *start* signal of the next, and hence the number of communication signals per unit of information is amortized to just one [1]. In $OOK$, an information value $v$ would be represented using approximately $\log_2 |S|$ bits, ($|S|$ is the cardinality of set $S$) where $v \in S$. As illustrated in Figure 3(a), a value of 5 is represented using 3 bits and requires $3t_b$ time units. However, in $TEC$, $v$ is represented using $v$ clock cycles, and hence the clock rate has to be exponentially larger than the underlying $OOK$ data-rate in order for $TEC$ to exhibit superior performance. Revisiting the set-up in Section III, for an $OOK$ data-rate of $3.8 * 10^{-5}$ bps and a clock rate of 1 Hz, under idealized channel conditions, $TEC$ will provide an average data-rate of $3.9 * 10^{-4}$ bps, a 10.3x improvement over $OOK$. In general, consider a decimal value $i$ being sent, the total delay required to communicate this data using $TEC$ is the sum of one bit period using molecular signaling and the information delay (say $t_{in} = \frac{i}{f_c}$) corresponding to the wait time for the data. Thus, it takes $TEC$ a maximum of $t_b + \frac{2^n-1}{f_c}$ time to transmit a $n$ bit data. The data-rate of $TEC$ is thus given by the following:

$$R_{tec} = \frac{n}{t_b + \frac{i}{f_c}} : i \in \{0, 1....2^n - 1\}. \qquad (1)$$

The notion of encoding information in time periods is not new to this work. *Timing channels* rely on such a notion to achieve covert information transfer [27], while *Pulse-Position Modulation (PPM)* relies

[1]Clocks are prevalent in bacteria. One naturally occurring example is the KaiABC system that control circadian rhythms in the bacterium *Synechococcus elongatus* [24]. Furthermore synthetic clocks have been generated and their rates altered by genetically manipulating *E. coli* bacteria to include genes from a variety of bacteria. [7], [21], [25]. Also, using bacteria for storage has been studied in synthetic biology. For e.g., in [26] researchers have developed rewritable storage using bacteria.

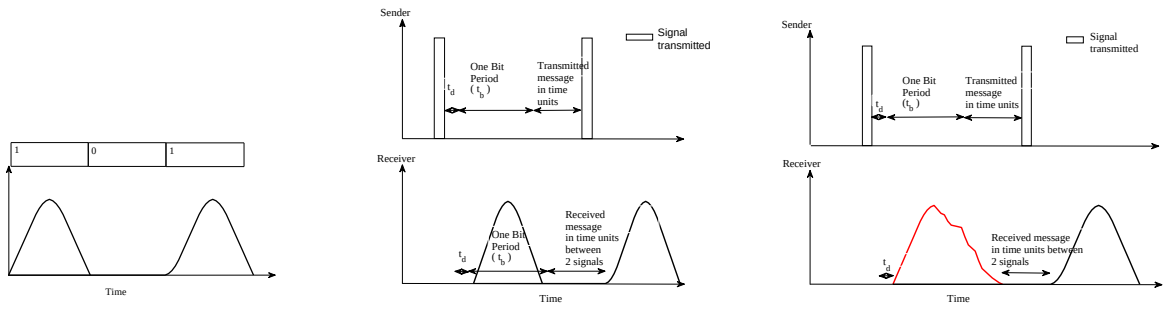


(a) OOK (b) TEC (c) TEC- Non zero error

Fig. 3: Illustration of modulation schemes

on conveying information through the relative position of pulses in environments where there is little or no error conditions. We discuss a few other related works later in the paper, but the key difference between such techniques and this work is significant: the domain of interest - bacterial communication - raises unique and considerable challenges in how a technique like $TEC$ can be realized in the target environment, and hence the solutions we propose to adapt $TEC$ are in turn unique and fundamentally tailored to the domain.

### A. Promise of TEC

We now use numerical analysis of the data-rate equations of $OOK$ and $TEC$ to study the promise of $TEC$ under variations of different parameters. Unless otherwise specified, we use a molecular signaling bit period $t_b$ of $435$ min based on the experimental results presented in Section III, and a clock rate of $1$ Hz. The data-rates of $OOK$ and $TEC$ as a function of the bit period $t_b$ is shown in Figure 4(a), while Figure 4(b) presents the relative performance improvement of $TEC$ with respect to $OOK$. With an increasing $t_b$, $TEC$'s improvement over $OOK$ increases since the dependency of $TEC$'s performance on the parameter is relatively smaller. Figure 4(c) presents the relative performance improvement of $TEC$ with respect to the number of bits $n$. It can be observed that the relative performance varies with $n$. Thus, for a given set of $t_b$ and $f_c$, there is an optimal value of $n$ that should be used in $TEC$. Finally, if the clock rate is higher, the waiting time between signals corresponding to the data value will be smaller. It can be observed from Figure 4(d) that $TEC$'s relative performance with respect to $OOK$ improves with higher $f_c$. Note that while a higher $f_c$ is always better under idealized zero error conditions, any skew in clock rates between the sender and the receiver will be exacerbated under realistic non-zero error conditions.

### B. Limitations of TEC

Thus far, we have explored the performance of $TEC$ under idealized zero error conditions. In reality, the responses of biological systems will vary across time. Figure 3(c) illustrates a deviation from ideal behavior. The start signal in Figure 3(c) gets delayed and hence the time elapsed between the signals is different leading to bit errors. To the best of our knowledge, there has not been any work that models the statistical distribution of the delay in the response of bacteria to molecular signals. Hence, we consider a simple uniform distribution $U\ (t_b\text{-}\epsilon, t_b\text{+}\epsilon)$ to model the real response time of receiver bacteria. On an average, one bit period is $t_b$ with a bounded error that is uniformly distributed $U(\text{-}\epsilon, +\epsilon)$. Any deviation from the average is termed as error. The net error $\epsilon$ is the sum of all errors from the time of introduction of molecules into the medium to the detection of fluorescence output. Given that the error is bounded, it is possible for the receiver to decode with 100% accuracy by the simple technique of increasing the minimum distance between messages. A message is defined by both the *start* and the *stop* signals, and both these signals can be subject to an error of $\pm\ \epsilon$. If the minimum distance between adjacent messages is at least $4\epsilon$, the receiver can decode messages correctly in spite of any errors. We refer to $TEC$ with simple error correction as $TEC\text{-}SIMPLE$. Figure 8(a) shows that the relative data-rate performance of $TEC\text{-}SIMPLE$

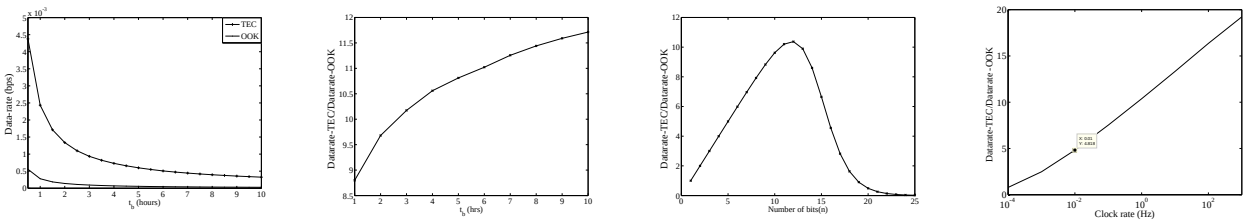


(a) Effect of Bit Period (b) Effect of Bit Period (c) Effect of Frame size (d) Effect of Clock rate

Fig. 4: Performance of $TEC$ under ideal zero error conditions

in a realistic system has reduced to approximately 1.8x $OOK$ (for an error of 10% in $t_b$). Thus, the introduction of error in the system has brought down the performance of $TEC$ considerably.

### *C. TEC-SMART : TEC for Non-Zero Error Conditions*

In this section we propose multiple techniques that in tandem improve the performance of $TEC$ under non-zero error conditions. Specifically, we present (i) an error curtailment/differentiation strategy that reduces the impact of error on $TEC's$ performance; (ii) a differential coding strategy that is uniquely targeted towards amortizing the cost of $t_b$ across multiple pieces of information; (iii) an optimization to the differential coding strategy that reduces overheads and (iv) an optimization to detect error in case of unbounded channel noise. We refer to a communication strategy that uses $TEC$ along with the aforementioned mechanisms as *smart time-elapse communication* ($TEC$-$SMART$).

*1)* **Error Curtailment/Differentiation:** The uniformly distributed error *U(-$\epsilon$,+$\epsilon$)* is actually the sum of multiple error components: propagation-time error $e_d$, rise-time error $e_r$, and fall-time error $e_f$ corresponding to the propagation of molecules through the medium, the ramp-up of fluorescence, and the ramp-down of fluorescence respectively. Instead of handling the composite error in its entirety, we propose handling the error in two independent stages by introducing redundancy in the *bit period* to handle $e_r$ and $e_f$, and by introducing redundancy in the *information delay* to handle $e_d$.

**Fall-Time Error Correction:** The time period between the end of the $i^{th}$ signal and the start of the $i + 1^{th}$ signal at the receiver represents the $i^{th}$ message. Any deviation from the estimated fall-time alters the stop of the current message, in-turn changing the absolute value of the data. Such an error in fall-time can be corrected by a proper choice of the sampling point. Assuming all other processes to be without error, it is sufficient to start measuring the time period in the rise phase of the receiver response and stop measuring upon the onset of the next rise phase. On subtracting $t_b$ from the total measured time, the actual message is retrieved. The fall-time error is thus absorbed in the time measurement phase. Such a correction can lead to inter-symbol interference (ISI). The first 2 output signals in Figure 5(a), illustrate interference between signals due to fall-time error in signal 1. To overcome ISI, the bit period is increased from $t_b$ to $t_b + e_f$. The last 2 output signals in Figure 5(a) have an increased bit period thus overcoming ISI.

**Rise-Time Error Correction:** The fall-time error correction was based on the assumption that all other timing components are error-free. An accurate ramp-up phase is thus essential in correcting fall-time error. If the propagation delay is error-free, the time at which the leading edge of signal reaches the receiver is error-free. Assuming that the propagation delay is error-free, the response of the receiver is extrapolated to identify the time at which leading edge of signal reached the receiver. The receiver adds (or subtracts) the difference between the actual and estimated times of arrival to its measure. Again, in order to ensure that two adjacent signals do not interfere, the bit period is further increased from $t_b + e_f$ to $t_b + e_f + e_r$. Figure 5(b) illustrates rise-time error and correction. The rise-time error in signal 1 causes interference between signals 1 and 2. Increase in bit period resolves this as seen in third and fourth signals in Figure 5(b). Thus, both rise and fall-time errors are corrected by simply increasing the bit period.

**Propagation Error Correction:** The propagation delay determines the time at which the leading edge of a signal reaches the receiver, which in turn

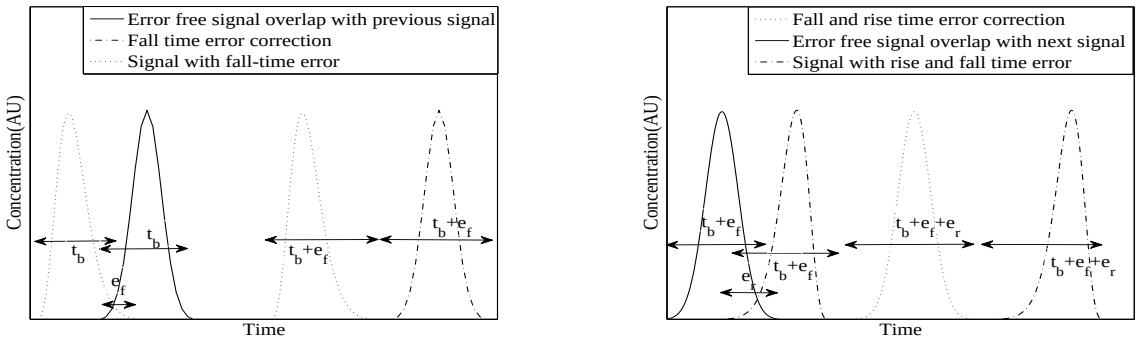


(a) Fall time error correction

(b) Rise time error correction

Fig. 5: Illustration of rise and fall time error correction

conveys the start of a message. Therefore, error in the propagation time is corrected by introducing redundancy in the message as in the simple error correction scheme with the minimum distance between messages being $4e_d$ instead of $4(e_d+e_f+e_r)$. If the first signal in a communication is error-free, it is possible to decode with zero error for a reduced minimum distance of $2e_d$ as every signal is corrected based on the received and decoded messages i.e., if the $start$ signal is received correct, only the $stop$ signal can be erroneous. Since we decode with 100% accuracy, the error introduced is predicted and the $stop$ is adjusted such that the error does not propagate. The transmission of first signal is restricted to slots of width one bit period ensuring an error-free start signal. In the following sections we assume the first signal to be error-free. The data-rate incorporating smart error correction mechanisms is as follows:

$$R_{tec} = \frac{n}{t_b + t_{in}}. \tag{2}$$

$TEC\text{-}SIMPLE$ performs error correction by multiplying each message by $2(e_d + e_f + e_r)$ enabling upto $e_d + e_f + e_r$ error correction. Therefore, the information delay($t_{in}$) is

$$t_{in} = \frac{i(2(e_d + e_f + e_r)f_c + 1)}{f_c} : i \in \{0, 1...2^n - 1\}.$$
$$R_{se} = \frac{n}{t_b + t_{in}}. \tag{3}$$

where, $R_{se}$ is the data-rate achieved using $TEC\text{-}SIMPLE$. Employing $TEC\text{-}SMART$, each message is multiplied by $2e_d$ while one bit period is increased from $t_b$ to $t_b + e_f + e_r$. The information delay in this case is given as,

$$t_{in} = \frac{i(2e_d f_c + 1)}{f_c} : i \in \{0, 1...2^n - 1\}.$$
$$R_{st} = \frac{n}{t_b + e_f + e_r + t_{in}}. \tag{4}$$

where, $R_{st}$ is the data-rate achieved using $TEC\text{-}SMART$ with only error differentiation.

*2)* **Differential Coding (DC):**
From Equation (3), it is evident that while curtailing the impact of error has a distinct benefit on the performance of $TEC$, the impact of $t_b$ still remains as-is. We thus propose a differential coding ($DC$) mechanism that leverages correlation between the values of consecutive messages to amortize the impact of $t_b$ across them. The messages at the source are assumed to be independent and identically distributed. Dependence is introduced by taking the differences of pairs of adjacent messages such that every message in the new sequence is smaller in value compared to that of the original. Since the message is encoded in time, the transmitted values cannot be negative. A sequence of *m* messages is hence arranged in increasing order, and a new sequence constituting differences between adjacent values is formed so that each element in the new sequence is positive and smaller than its value in the original sequence.

Since the ordering of elements in the original sequence is altered by virtue of the rearrangement, the actual order must be transmitted as a separate message. If a table of different orders is shared by the end systems, where the table has all possible orders for $m$ messages (i.e., $m!$ entries), a message

of size $\lceil \log_2 m! \rceil$ bits is required to transmit the order. Consider an example to understand the aspects of $DC$. Let the messages to be transmitted by the source be 10(0), 30(1), 5(2), 25(3), 3(4) where the numbers in the bracket denote the position of the message in the sequence. Differential coding is performed in 2 steps. In step 1, the messages are arranged in increasing order. Here, in this example it is 3(4), 5(2), 10(0), 25(3), 30(1). The ordered messages are then passed through differential encoder block that takes difference of adjacent messages giving an output 3, 2, 5, 15, 5 for the above example. Since the messages are arranged in increasing order, the sequence at the output of differential encoder contains only positive values. The position of corresponding order in the table maintained by end systems is transmitted as another message. Let us say the order 4,2,0,3,1 is at position 10 in the table. In this example, the total delay is "40" clock ticks+6$t_b$ as against the "73" clock ticks+5$t_b$ without coding. The number of clock ticks per message is reduced with the use of $DC$ that in turn translates to a higher data-rate.

The sum of elements in the new sequence is equal to the largest element in the original sequence and hence the total waiting time is the sum of the waiting time to transmit the largest message in the sequence and the corresponding ordering. Let $M = \{m_1, m_2 ... m_m\}$ be the sequence of messages to be transmitted. The information delay per sequence $M$, $t_{dc}$ is

$$t_{dc} = \frac{(max(M) + j)(2e_d f_c + 1)}{f_c} \quad (5)$$
$$: m_i \in \{0, 1....2^n - 1\} \text{ and } m_i \in M$$
$$: j \in \{0, 1...m! - 1\}$$

$$R_{dc} = \frac{mn}{(m+1)(t_b + e_f + e_r) + t_{dc}} \quad (6)$$

where $R_{dc}$ is the data-rate achieved using $DC$. The receiver has to wait till the end of sequence to receive all $m$ messages. Thus, the delay in $DC$ is higher than that in $TEC\text{-}SMART$ without coding but is close to that of $OOK$. For an $n$-bit message, $OOK$ takes $nt_b$ time units while $DC$ transmits $mn$ bits in a maximum of $mt_b$+ $t_{in}$ time units. The delay in $DC$ is close to $nt_b$ units if $m$ is close to $n$ (as $t_{in} \ll t_b$). It has been observed that $m$ is close to $n$ over different values of $t_b$.

*3)* **Piggybacked Ordering ($\mathbf{DC_P}$):**
Recall that $DC$ adds one extra message per sequence to convey the ordering of messages in the sequence. $DC_P$ is an optimization technique that eliminates the extra message in $DC$ for conveying the ordering of messages. We refer to this variant as $TEC\text{-}SMART(DC_P)$. To keep the number of signals equal to the number of messages, the order is conveyed embedded within the message. Thus, one pair of (bit period + delay corresponding to order) is eliminated at the cost of increased waiting time per message. Every message (the difference) is multiplied by a constant $k_1$ and a portion of the ordering information is added. Redundancy in information delay and bit period is then introduced to the resultant message for error correction. The receiver, after performing error correction divides the number by the same constant $k_1$ so that the quotient is the message and the remainder is the portion of ordering. In this fashion, the receiver is able to recreate the ordering message that is embedded in the data messages. The order embedded in each message is $k_2$. The information delay in case of $DC_P$ is,

$$t_{dcp} = \frac{(max(M)k_1 + k_2)(2e_d f_c + 1)}{f_c}$$
$$: m_i \in \{0, 1....2^n - 1\} \text{ and } m_i \in M \quad (7)$$

$$R_{DC_P} = \frac{mn}{m * (t_b + e_f + e_r) + t_{dcp}} \quad (8)$$

where $R_{DC_P}$ is the data-rate achieved using $DC_P$. The constant $k_1$ is chosen such that $log_2 k_1 \geq \frac{\log_2 m!}{m}$ i.e., the constant should be able to indicate the number of extra bits per message to represent the order. Considering m = 8, the number of bits required to represent $8!$ is 16 and hence 2 *bits per message* making $k_1 = 4$. $k_1$ cannot be arbitrarily large; the larger the value of $k_1$, the higher the waiting delay per message. An optimization to choose the best possible value of $k_1$, given $t_b$ and $m$ must be performed.

*4)* **DC for unbounded noise - $\mathbf{DC_U}$:**
We proposed $TEC\text{-}SMART$, that uses error differentiation and piggybacked ordering to improve data-rate performance in a bounded noise channel. We considered a simple case of uniformly distributed additive channel noise. In this section, we analyze $TEC\text{-}SMART$ in the case of unbounded noise. We propose an optimization to detect error in an unbounded noise channel. When noise distribution is unbounded, it is not possible to achieve 100% error correction. We propose $DC_U$ as an optimization

that can detect error in case of unbounded noise. $DC_U$ gives a percentage of correctable, detectable and undetectable error for a given noise distribution. In the rest of the paper, we refer to this variant as $TEC\text{-}SMART(DC_U)$.

As described in Section IV-C3, $TEC\text{-}SMART(DC_P)$ requires the sender and receiver to share a list of ordering. For a sequence of $m$ messages, a list of $m!$ entries is shared by sender and receiver. The location of order in the list is appended to the actual message. Noise in the channel alters the location of the order and not the actual ordering. As every received location maps to a valid order, a timing error more than $\epsilon$ cannot be detected.

$TEC\text{-}SMART(DC_U)$ detects errors by appending the absolute ordering to the message. In order to represent the order of $m$ messages, each message requires an additional $\log_2 m$ bits. The order in each message is distinct and takes only values from 1 to $m$. Each message in the new sequence is then multiplied by $2\epsilon$. If the error is greater than $\epsilon$, the order appended is changed. Absence of $m$ unique order at the receiver indicates an uncorrected error. $DC_U$ also avoids the need for a list of order to be shared by sender and receiver. No extra memory is required. Thus, if an error greater than $\epsilon$ is added to the message, the order as decoded by receiver will not have $m$ distinct numbers thus indicating the presence of an error. In the following conditions, error detection is not possible:

1) Error in each message such that there are $m$ distinct orders but at different positions
2) Large enough $\epsilon$ such that order still remains but message is altered

For a sequence of $m$ messages, there are $m!$ distinct ordering, of which only one is correct. There will be $m! - 1$ possibilities of wrong reception with $DC_U$. But the total number of erroneous reception can be $m^m$ . Of the $m^m$ possibilities, $m! - 1$ cannot be detected. The rest can be detected. $\frac{m!-1*100}{m^m}$ gives the percentage undetectable error. The choice of $\epsilon$ determines the percentage of correctable error and choice of $m$ determines the percentage of detectable error.

*5)* **Summary:**
Thus far in this section we have presented $TEC\text{-}SMART$, a communication approach to improve data-rate performance of bacterial communication under non-zero error conditions. In the following sections, we use both theoretical and numerical analysis to evaluate $TEC\text{-}SIMPLE$ and $TEC\text{-}SMART$.

## V. Capacity Analysis

Capacity of a channel is given by the maximum mutual information $I(X:Y)$ between input X and output Y, maximized over all input distributions.

$$C = \lambda \max_{f_X(x)} I(X:Y) \tag{9}$$

where, $\lambda = \frac{1}{E(Y)}$ is the inter-arrival rate at the receiver. To the best of our knowledge, existing works do not characterize the channel delay of a molecular communication system. We broadly classify channel delay into *bounded* and *unbounded* noise. Among bounded noise distributions, uniform distribution results in lowest data-rate as all delay components have equal probability. Following queueing theory, exponential service distributed timing channel provides the worst case data-rate performance. Therefore, following the approach in [28], we derive the maximum achievable data-rate for uniform and exponential distribution of channel delay.

### A. Uniform Distribution

Let N be the channel delay. N is uniformly distributed with mean $t_b$. $N \sim U(t_b - \epsilon, t_b + \epsilon)$. Since information is conveyed in time intervals, there is no parameter analogous to signal power [29]. Therefore, constraint on the input can be mean or peak. Let X be the inter-arrival delays at the sender end and Y be the inter-arrival delays at the receiver end. Consider $x_1 \in X$ be the message to be transmitted. Due to the response time at receiver bacteria, the receiver observes $y_1 \in Y$ as $y_1 = x_1 + N_1$, where $N_1 = t_b + n_1$ is the error introduced by the channel and $t_b$ is the average time required by bacteria to respond to a signal. Upon reception, the receiver subtracts the average response time of receiver from the observed time and the received message is $y_1 - t_b$. Thus, the system can be modeled using the following equation,

$$Y = X + N - t_b \tag{10}$$

We derive the capacity of timing channel using differential entropy of Y and N.

$$I(X:Y) = h(Y) - h(Y|X) \tag{11}$$

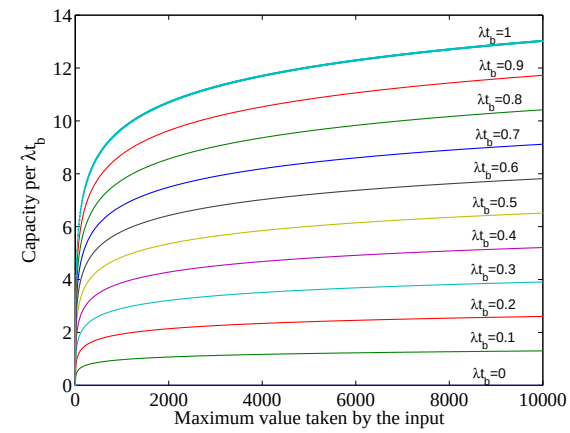


(a) Bounded channel delay with peak-constrained input

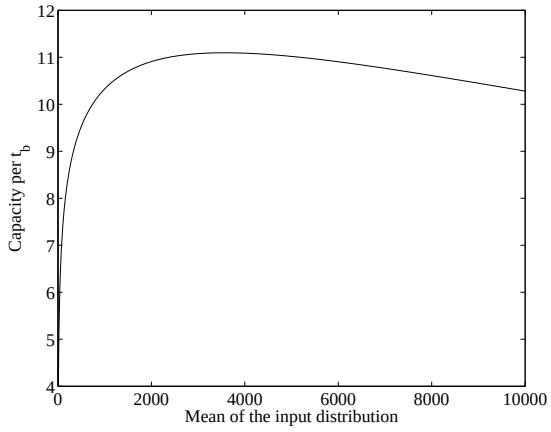


(b) Bounded channel delay with mean-constrained input

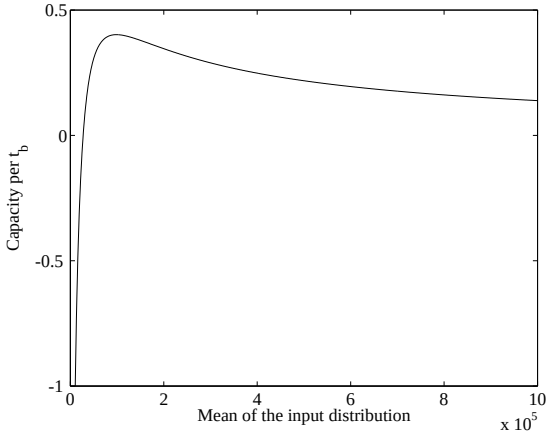


(c) Unbounded channel delay with mean-constrained input

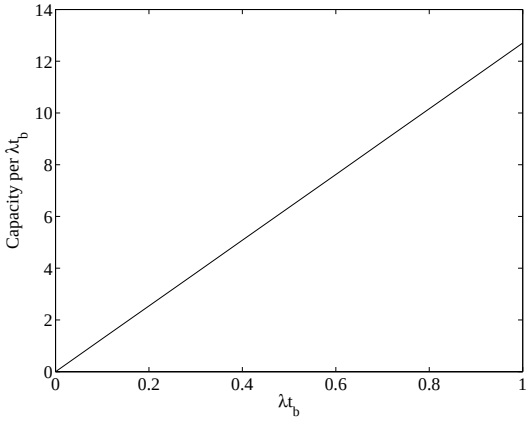


(d) Bounded channel delay for a given input mean

Fig. 6: Theoretical analysis of capacity

$$= h(Y) - h(X+N|X) \quad (12)$$

$$h(X+N|X) = h(N|X) \quad (13)$$

as X and N are independent

$$I(X:Y) = h(Y) - h(N|X) \quad (14)$$

$$= h(Y) - h(N) \quad (15)$$

*Case 1: Peak-Constraint:* X $\backsim$ [0,$t_x$]. Since X and N are bounded, Y is also bounded. [30] shows that among all bounded distributions, uniform distribution is the entropy maximizing distribution. $Y \sim U(-\epsilon, t_x + \epsilon)$. The differential entropy of uniform distribution is given by, $h(Y) = \ln(t_x + 2\epsilon)$ and $h(N) = \ln(2\epsilon)$. Substituting in Equation 11,

$$I(X:Y) = \ln(t_x + 2\epsilon) - \ln(2\epsilon) \quad (16)$$

$$C \leq \lambda \ln \frac{t_x + 2\epsilon}{2\epsilon} \quad (17)$$

Capacity per average delay of channel is obtained by,

$$C \leq \lambda t_b \ln \frac{t_x + 2\epsilon}{2\epsilon} \quad (18)$$

where, $\lambda$=$\frac{1}{t_b + E(Y)}$ is the average inter-arrival rate at the receiver. Since $E(Y) \geq 0$, $\lambda t_b$ varies from 0 to 1. As shown in Figure 6(a), maximum capacity is achieved when $\lambda t_b = 1$. Also, capacity increases with increasing $t_x$. Note that $\lambda t_b$ is strictly less than 1, as $E(Y) = E(X)$ and $E(X) \geq 0$. The different colors in 6(a) denote different values of $\lambda t_b$. For a given $t_x$, depending on the error correction mechanism and modulation, the system approaches a certain ratio of $\lambda t_b$. The higher the value of $\lambda t_b$ is, the better the algorithm is, in achieving the maximum data-rate. The smaller the value of $E(X)$, higher the ratio $\lambda t_b$ i.e., for small values of $E(X)$, $E(Y) \approx t_b$. The delay at the receiver end is thus

dominated by bit period leading to an increased data-rate.

If $\epsilon << t_x$, then an approximation for entropy maximizing input distribution can be derived. Assume $X \sim U(0, t_x)$. We assumed $N \sim U(t_b - \epsilon, t_b + \epsilon)$. The distribution of sum of 2 independent random variables is the convolution of 2 distributions [31]. Here, both $X$ and $N$ are uniformly distributed. Convolution of these 2 uniform pulses gives a trapezium. The slope of the sides of the trapezium is very high if $\epsilon << t_x$, which we can approximate to a uniform distribution. Hence, for peak constrained input in a uniform noise distribution channel such that $\epsilon << t_x$, uniformly distributed input maximizes channel capacity.

*Case 2: Mean-Constraint:* $E(X) \leq k$ where $k$ is an arbitrary constant. The mean of the input distribution is constrained. Since $Y = X + N - t_b$, $E(Y) = E(X)$, Y is also mean-constrained. Note that $Y + t_b$ is the time between 2 receptions and hence is positive. Among all mean-constrained, positive distributions, exponential distribution gives the maximum entropy. Thus, capacity is upper bounded when $Y + t_b$ and hence $Y$ follows exponential distribution. Since entropy does not change with linear translation, $h(Y) = 1 - \ln \frac{1}{E(Y)}$. Similar to case 1,

$$I(X:Y) = 1 - \ln \frac{1}{E(Y)} - \ln(2\epsilon) \tag{19}$$

as E(Y)=E(X),

$$C \leq \lambda(1 + \ln \frac{E(X)}{2\epsilon}) \tag{20}$$

Total delay per reception is $E(Y) + t_b$. Thus, the capacity per average delay of channel is,

$$C \leq \lambda t_b(1 + \ln \frac{E(X)}{2\epsilon}) \tag{21}$$

Figure 6(b) shows the capacity as a function of mean of the input with $t_b = 435$min and $\epsilon = 0.6$s. With increasing mean, the capacity increases to a maximum and then decreases. Till the peak, total delay is dominated by $t_b$ after which, the delay increases linearly whereas the number of bits represented increases logarithmically. Thus the net data-rate decreases.

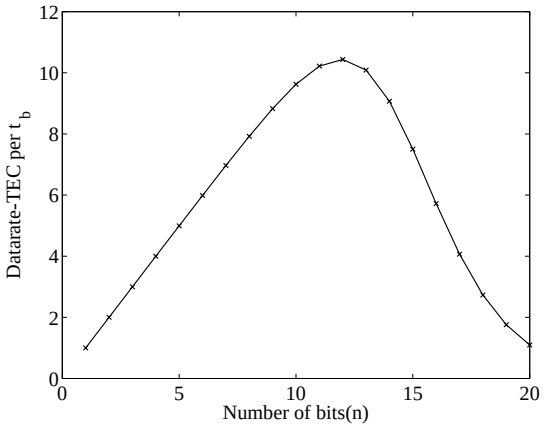


Fig. 7: Simulation based capacity

### B. Exponential Distribution

In case of unbounded distribution, peak-constraint for input is not tractable. Therefore, we consider a mean-constrained input. Let N $\sim$ Exp($\frac{1}{t_b}$). Following the case 2 of uniformly distributed noise, Y should follow exponential distribution with mean $E(Y) = E(X)$.

$$I(X:Y) = 1 - \ln \frac{1}{E(Y)} - 1 + \ln \frac{1}{t_b} \tag{22}$$

$$C \leq \lambda \ln \frac{E(X)}{t_b} \tag{23}$$

Capacity per average delay of channel is obtained by,

$$C \leq \lambda t_b \ln \frac{E(X)}{t_b} \tag{24}$$

Following the theoretical analysis, the maximum achievable data-rate under different constraints on input distribution for uniform and exponential noise distribution has been derived. The performance of proposed error correction scheme along with timing modulation is compared against channel capacity. The simulation results do not include the differential encoder block as data-rate across channel is compared. Figure 7 shows the data-rate performance based on simulation results. The results show that the proposed error correction has $10.5X$ improvement over OOK with peak constraint on input at $2^{12}$. The input and the noise were uniformly distributed. Under the given conditions, maximum achievable capacity is $11.7X$ over OOK. The data-rate of the proposed solution is 90% of that of the maximum achievable data-rate.

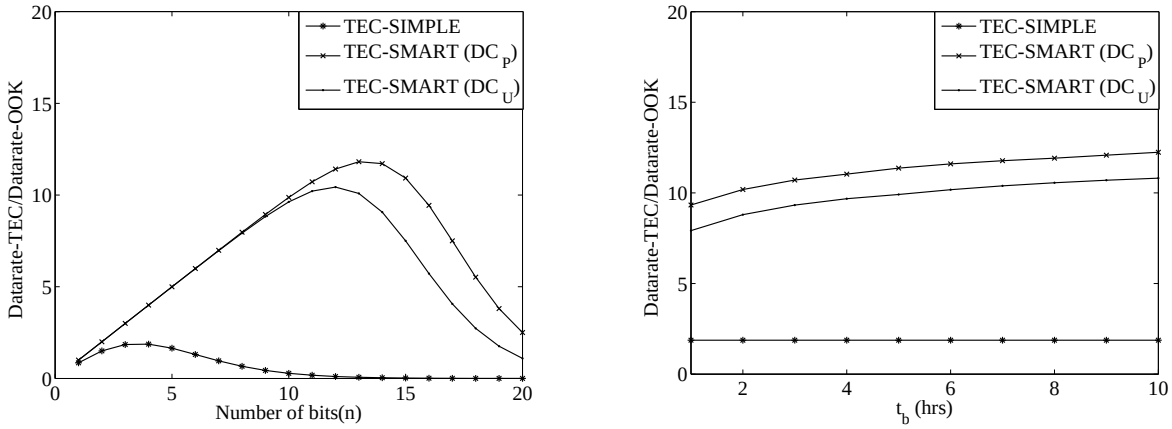


(a) Effect of Frame size

(b) Effect of Bit period

Fig. 8: Performance of $TEC$-$SMART$ and $TEC$-$SIMPLE$ with varying $n$ and $t_b$

## VI. Numerical Analysis

We present the receiver design and the numerical analysis of $TEC$ in this section.

### *Receiver Design*

The receiver bacterial colony fluoresce on reception of AHL signal. The first AHL signal is the $start$ signal and triggers the counter [2] at receiver to start counting. At the reception of next AHL signal, the counter is reset and the clock count is stored as $y$. The bit period, rise-time and fall-time error ($t_b$+$e_f$+$e_r$) is subtracted from $y$. $y_1 = y - t_b - e_f - e_r$. Then, the message is corrected for diffusion error by, $y_2 = \frac{y_1}{2e_d}$ as we multiplied the message by $2e_d$ before transmission. In a bounded noise channel, $y_2$ is 100% error-free. In an unbounded channel noise, error greater than $\epsilon$ cannot be corrected. $y_2$, which has been corrected for error is then divided by $\log_2 m!$, the remainder of which gives the index of order (in case of $DC_U$ it gives the order itself) and the quotient gives the difference of messages. Each message is then obtained by taking sum of differences. Based on the order, the messages are then re-ordered. In case of $DC_U$, if order is not unique, then we can detect that an error more than $\epsilon$ has been added.

[2]The basic building blocks of a processor are transistors and logic gates. [32] illustrates implementation of logic gates using bacteria. In the future, we can use these blocks to build the processing unit at sender and receiver.

### *Evaluation*

We now perform numerical analysis of Equations (1) to (7) using MATLAB. The specific values for the parameters and the ranges for parameters used are driven by the experimental results presented in Section III. Unless otherwise specified we use the following values: $t_b$ =435 min, $t_d$ =6 sec, $e_f + e_r = 0.1t_b$, $e_d = 0.1t_d$. Since the performance of $TEC$-$SMART$ is dependent on the message size, the bit period, error introduced by the channel and the clock rate, we study the sensitivity of its performance to these different parameters. We present only relative performance results for $TEC$ and its variants with respect to $OOK$. Every data point is obtained by taking an average of data-rate corresponding to all messages of frame size $n$.

### A. Frame Size

Unlike other modulation techniques, the data-rate of $TEC$ varies with the frame size $n$. The total delay for a transmission varies with the absolute value of the message. For small values of *n*, information delay $t_{in} << t_b$. Thus, the data-rate increases with increasing *n*. Once $t_{in}$ is comparable to $t_b$, the data-rate begins to decrease as the $t_{in}$ starts dominating. The relative data-rate performance of $TEC$ is presented in Figure 8(a). This motivates the need for an appropriate selection of $n$ given a target environment. The performance of $TEC$-$SMART(DC_U)$ is for an unbounded channel delay distribution. The goal of $TEC$-$SMART(DC_U)$ is to detect error in the presence of unbounded noise

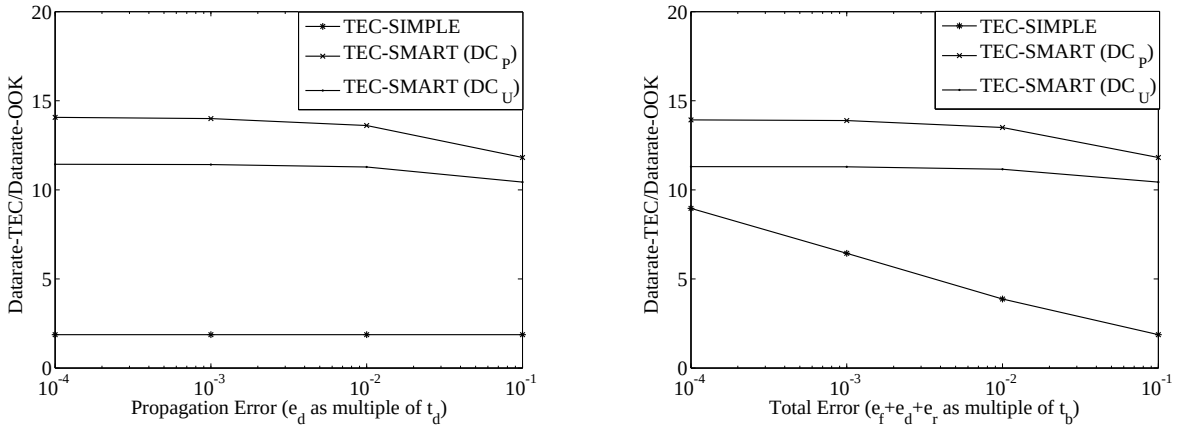


(a) Effect of Propagation error

(b) Effect of Total error

Fig. 9: Performance of $TEC\text{-}SMART$ and $TEC\text{-}SIMPLE$ under varying error conditions.

and hence the maximum data-rate achievable is smaller than $TEC\text{-}SMART(DC_P)$, which cannot correct or detect any error greater than $e_d$.

### B. Bit Period

Figure 8(b) presents the data-rate performance for $TEC$, $TEC\text{-}SMART(DC_P)$ and $TEC\text{-}SMART(DC_U)$ for different bit period. The value of $t_b$ is varied from 1 to 20 hours. It can be observed from the results that while $TEC$ is impacted heavily in its performance by an increase in $t_b$, $TEC\text{-}SMART(DC_P)$ and $TEC\text{-}SMART(DC_U)$ is considerably more resilient to larger values of $t_b$. This is due to the amortization of the $t_b$ overhead over multiple messages.

### C. Frequency

Figure 4(d) shows an increase in the data-rate with increasing clock frequency. With the introduction of error in the system, the clock rate loses its significance. Recall that the transmitter and the receiver measure the number of $e_d$ time units between the start and stop signals. Hence, however high the clock rate is, the time slot is now in terms of error and hence the data-rate performance does not change with frequency once the error correction is introduced.

### D. Error

We proposed $TEC\text{-}SMART$ as a better error correction strategy. $TEC\text{-}SMART$ considers both bounded and unbounded error and proposes strategies to detect uncorrected error with high probability in case of unbounded error. We analyze the performance of $TEC\text{-}SMART$ under bounded and unbounded error for varying error conditions.

*Bounded Error:* Recall from Section IV that the performance of $TEC\text{-}SIMPLE$ reduced to being marginally better than that of $OOK$ under non-zero error conditions. However, $TEC\text{-}SMART$ is explicitly designed to handle error conditions better by virtue of its error curtailing and differentiation mechanisms. Thus, the increase in *rise-time error* and *fall-time error* has minimal impact on the overall performance of $TEC\text{-}SMART$. In this section, we analyze the results in a bounded error. As seen in Figure 9(a), $TEC\text{-}SMART(DC_P)$ can deliver a data-rate of over 10x even when the total error is large ($0.1t_b$+$e_d$). Data-rate with respect to varying error components is presented in Figures 9(a)-9(b). Overall, the results demonstrate the better error resiliency exhibited by $TEC\text{-}SMART(DC_P)$.The data-rate delivered by $TEC\text{-}SMART(DC_U) < TEC\text{-}SMART(DC_P)$ but the former can detect error greater than $e_d$.

*Unbounded Error:* In the case of positive valued unbounded channel delay, exponential distribution can be considered as a general case, similar to Gaussian distribution in energy based communication. Figure 10 shows the performance of $TEC\text{-}SMART(DC_U)$ under exponential channel delay. The percentage of correctable error is increased by increasing $\epsilon$ but this reduces the data-rate due to the increase in redundancy. Figure 10(b) shows

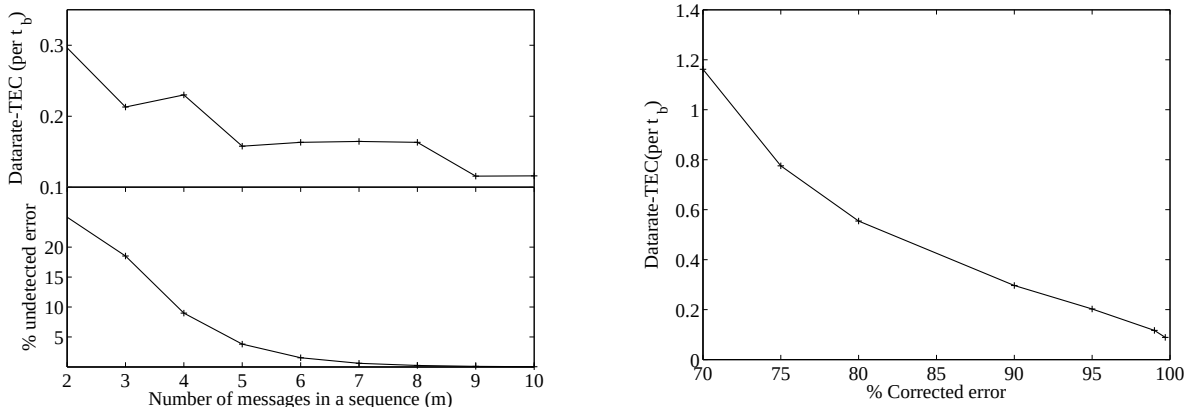


(a) Effect of Number of messages per sequence on datarate

(b) Effect of Propagation error on datarate

Fig. 10: Performance of $TEC\text{-}SMART(DC_U)$ under exponential noise in the channel.

the decrease in data-rate with increasing $\epsilon$. The following analysis is used to estimate $\epsilon$ for a given $\%$ of error correction. Let $a$ be the fraction of error to be corrected and $f(x)$ be the probability distribution of exponential error. For e.g, $a = 0.9$ for 90% error correction

$$\int_0^{\epsilon} \mathrm{f(x)}\,\mathrm{d}x = a.$$

For an exponential distribution,

$$F(\epsilon) = a$$

where, F(x) is the cumulative distribution function

$$1 - e^{-\lambda\epsilon} = a$$
$$\epsilon = -\lambda(ln(1-a))$$

Figure 10(a) shows the variation of data-rate and percentage of undetected error with increasing $m$. The correctable error is set to 90%. The value of $\epsilon$ to be multiplied to the message is obtained from the probability distribution of channel noise as explained above.

From the capacity analysis and numerical analysis, we observe that $TEC$ is suitable for *super-slow networks*. Depending on the application and the target environment, the optimum value of $n$, $\epsilon$ and $m$ for a given $t_b$ is identified a priori using the analysis presented above. In a bounded error, $TEC$ provides over an order of magnitude improvement over $OOK$ in data-rate performance while in an unbounded error, it can still detect uncorrected error.

## VII. Related work

In addition to timing channels and PPM identified in SectionIV, there are few other approaches related to $TEC$. However, these approaches do not cater to the large error-rate or bit periods of the target bacterial communication environment, We discuss some of these approaches below:

**Timing Channels:** In [33] mechanisms to improve the data-rate of timing channel have been proposed. However, the proposed techniques are not targeted for the context of bacterial communication. Specifically, this work involves the use of static and complex coding tables unsuitable for the target environment. More importantly, it does not deal with large error rates and hence will perform similar to $TEC$ without any optimization.

**Communication through Silence:** [34] uses silent periods in sensor networks to communicate. The primary goal is to reduce the energy consumption, but error conditions are not considered. Also, data-rate improvement is not the primary focus.

**Timing modulation in fluid channel:** [29] presents an information theoretic approach to the timing modulation in molecular communication. Absolute timing is relied upon and hence it requires strict clock synchronization. Further, data-rate improvement is not a focus of this work.

## VIII. Conclusions

In this paper, using state-of-art advancements in genetic engineering and microfluidics we have argued with results from an experimental test-bed that a modulation technique like $OOK$ is indeed

achievable for communication between bacterial populations relying on molecular signaling. We also have shown that the data-rate performance of $OOK$ is extremely low because of the large bit periods. We propose a communication strategy called time-elapse communication with a set of optimization mechanisms that improves the data-rate over $OOK$ by more than an order of magnitude. We derived the maximum achievable capacity of time based communication for a uniformly distributed noise and an exponentially distributed noise channel.

## REFERENCES


[1] I. F. Akyildiz and J. M. Jornet, "Electromagnetic wireless nanosensor networks," *Nano Communication Networks*, 2010.

[2] G. Deligeorgis, M. Dragoman, D. Neculoiu *et al.*, "Microwave propagation in graphene," *Applied Physics Letters*, 2009.

[3] T. Suda, M. Moore, T. Nakano, R. Egashira, A. Enomoto, S. Hiyama, and Y. Moritani, "Exploratory research on molecular communication between nanomachines," in *GECCO 2005*.

[4] A. W. Eckford, "Molecular communication: Physically realistic models and achievable information rates," *arXiv:0812.1554v1*.

[5] I. F. Akyildiz, F. Fekri, C. R. Forest, B. K. Hammer, and R. Sivakumar, "Monaco: Fundamentals of molecular nano-communication networks (invited paper)," *IEEE Wireless Communications Magazine, Special Issue on Wireless Communications at the Nano-Scale*, 2012.

[6] N. Farsad, A. Eckford, S. Hiyama, and Y. Moritani, "On-chip molecular communication: Analysis and design," *NanoBioscience, IEEE Transactions on*, 2012.

[7] T. Danino, Mondragon-Palomino, Octavio, Tsimring *et al.*, "A synchronized quorum of genetic clocks." *Nature*, 2010.

[8] D. Endy, "Foundations for engineering biology," *Nature*, vol. 438, no. 7067, pp. 449–453, 1111.

[9] B. L. Bassler, "How bacteria talk to each other: regulation of gene expression by quorum sensing," *Current Opinion in Microbiology*, 1999.

[10] P. Melke, P. Sahlin, A. Levchenko, and H. Jönsson, "A cell-based model for quorum sensing in heterogeneous bacterial colonies," *PLoS Computational Biology*, 2010.

[11] T. Charrier, C. Chapeau, L. Bendria *et al.*, "A multi-channel bioluminescent bacterial biosensor for the on-line detection of metals and toxicity. Part II: technical development and proof of concept of the biosensor," *Analytical and Bioanalytical Chemistry*, 2011.

[12] J. Stocker, D. Balluch, Gsell *et al.*, "Development of a set of simple bacterial biosensors for quantitative and rapid measurements of arsenite and arsenate in potable water," *Environmental Science & Technology*, 2003.

[13] J. Engebrecht, K. Nealson, and M. Silverman, "Bacterial bioluminescence: Isolation and genetic analysis of functions from *Vibrio fischeri*," *Cell*, vol. 32, no. 3, pp. 773 – 781, 1983.

[14] J. Sambrook, *Molecular Cloning: A Laboratory Manual, Third Edition (3 volume set)*, 3rd ed., Jan. 2001.

[15] F. R. Blattner, G. Plunkett, Bloch *et al.*, "The complete genome sequence of *Escherichia coli* k-12." *Science*, 1997.

[16] J. B. Andersen, C. Sternberg, Poulsen *et al.*, "New unstable variants of green fluorescent protein for studies of transient gene expression in bacteria." *Applied and environmental microbiology*, vol. 64, no. 6, pp. 2240–2246, Jun. 1998.

[17] J. R. van der Meer and S. Belkin, "Where microbiology meets microengineering: design and applications of reporter bacteria," *Nature Reviews Microbiology*, 2010.

[18] R. D. Whitaker, S. Pember, B. C. Wallace, C. E. Brodley, and D. R. Walt, "Single cell time-resolved quorum responses reveal dependence on cell density and configuration," *Journal of Biological Chemistry*, vol. 286, 2011.

[19] A. Meyer, J. A. Megerle, C. Kuttler, J. Müller, C. Aguilar, L. Eberl, B. A. Hense, and J. O. Rädler, "Dynamics of AHL mediated quorum sensing under flow and non-flow conditions." *Phys Biol*, vol. 9, no. 2, p. 026007, 2012.

[20] S. Park, X. Hong, W. S. Choi, and T. Kim, "Microfabricated ratchet structure integrated concentrator arrays for synthetic bacterial cell-to-cell communication assays," *Lab Chip*, vol. 12, pp. 3914–3922, 2012.

[21] A. Prindle, P. Samayoa, I. Razinkov *et al.*, "A sensing array of radically coupled genetic 'biopixels'." *Nature*, 2012.

[22] A. Groisman, C. Lobo, H. Cho, J. K. Campbell, Y. S. Dufour, A. M. Stevens, and A. Levchenko, "A microfluidic chemostat for experiments with bacterial and yeast cells," *Nature methods*, vol. 2, no. 9, pp. 685–689, Sep. 2005.

[23] J. R. Anderson, D. T. Chiu, H. Wu, O. J. Schueller, and G. M. Whitesides, "Fabrication of microfluidic systems in poly(dimethylsiloxane)," *ELECTROPHORESIS*, Jan. 2000.

[24] P. Lenz and L. Søgaard-Andersen, "Temporal and spatial oscillations in bacteria," *Nature Reviews Microbiology*, 2011.

[25] O. Mondragón-Palomino, T. Danino, J. Selimkhanov, L. Tsimring, and J. Hasty, "Entrainment of a population of synthetic genetic oscillators," *Science*, vol. 333, no. 6047, pp. 1315–1319, 2011.

[26] J. Bonnet, P. Subsoontorn, and D. Endy, "Rewritable digital data storage in live cells via engineered control of recombination directionality," *Proceedings of the National Academy of Sciences*, 2012.

[27] V. Anantharam and S. Verdú, "Bits through queues," *IEEE Transactions on Information Theory*, 1996.

[28] S. Sellke, N. B. Shroff, S. Bagchi, and C.-C. Wang, "Timing channel capacity for uniform and gaussian servers," in *Forty-Fourth Annual Allerton Conference on Communication, Control, and Computing*, 2006.

[29] K. V. Srinivas, A. W. Eckford, and R. S. Adve, "Molecular communication in fluid media: The additive inverse gaussian noise channel," *IEEE Transactions on Information Theory*, 2012.

[30] T. M. Cover and J. A. Thomas, *Elements of Information Theory (Wiley Series in Telecommunications and Signal Processing)*.

[31] A. Papoulis and U. S. Pillai, *Probability, Random Variables and Stochastic Processes*, Dec. 2001.

[32] B. Wang, R. I. Kitney, N. Joly, and M. Buck, "Engineering modular and orthogonal genetic logic gates for robust digital-like synthetic biology," *Nature communications*, vol. 2, p. 508, 2011.

[33] S. Sellke, C. Wang, S. Bagchi, and N. Shroff, "TCP/IP timing channels: Theory to implementation," *INFOCOM*, 2009.

[34] Y. Zhu and R. Sivakumar, "Challenges: communication through silence in wireless sensor networks," in *MobiCom*, 2005.